Light quasiparticles dominate electronic transport in molecular crystal field-effect transistors

Z.Q. Li[1*], V. Podzorov[2], N. Sai[1,3], M.C. Martin[4], M.E. Gershenson[2], M. Di Ventra[1], and D.N. Basov[1]

[1] Department of Physics, University of California, San Diego, La Jolla, California 92093, USA
[2] Department of Physics and Astronomy, Rutgers University, Piscataway, New Jersey 08854, USA
[3] Department of Physics, The University of Texas at Austin, Austin, Texas 78712, USA
[4]Advanced Light Source Division, Lawrence Berkeley National Laboratory, Berkeley, California 94720, USA
*e-mail: zhiqiang@physics.ucsd.edu

A comprehensive understanding of charge transport in organic semiconductors poses a significant intellectual challenge and, at the same time, is crucial for further advances in the field of "plastic electronics"[1-3]. One longstanding problem pertains to the nature of excitations responsible for charge transport in these systems[4-6]. Here we report on an infrared spectroscopy study of mobile holes in the accumulation layer of organic field-effect transistors based on rubrene single crystals. Our data indicate that both transport and infrared properties of these transistors at room temperature are governed by light quasiparticles in molecular orbital bands with the effective masses m* comparable to free electron mass. Furthermore, the m* values inferred from our experiments are in agreement with those determined from band structure calculations. These findings reveal no evidence for prominent polaronic effects, which is at variance with the common beliefs of polaron formation[4, 5] in molecular solids.

Organic electronics is experiencing a surge of activities worldwide motivated by the potential applications of organic semiconductors in low-cost, large-area and flexible electronic devices, as well as basic scientific interest[1-3]. Despite the intensive research efforts in this field, the microscopic nature of charge carriers in organic semiconductors is still not well understood. A commonly used description of charge transport in organic molecular crystals[4, 5] is that the electrical current in these easily polarizable materials is carried by polarons: electrons or holes strongly coupled to local lattice deformations. A hallmark of the polaronic transport is a strong enhancement of the effective mass m* compared to the band values[4, 5]. Therefore, the hypothesis of polaron formation in molecular crystals is verifiable since the effective masses of mobile charges can be directly probed in infrared (IR) spectroscopic measurements. Here we report on IR spectroscopy studies of charge carriers in the conducting channel of organic field-effect transistors (OFET) based on single crystals of rubrene ($C_{42}H_{28}$, Fig.1b inset), a small-molecule organic semiconductor[6-9]. These studies show that charge transport in rubrene based OFETs at room temperature is dominated by light quasiparticles in the highest occupied molecular band (HOMO). New spectroscopy data along with the analysis of the electronic structure help to elucidate recent observations of non-activated, diffusive charge transport at the surface of high-quality molecular crystals in studies of *single-crystal* OFETs[6-9].

We start by examining the transmission spectrum T(ω) of a bare rubrene single crystal (Fig. 1b) since these spectra will be instructive for the understanding of the response of rubrene-based field-effect transistors. The sharp absorption lines below 5000 cm^{-1} originate from phonons in rubrene. The abrupt suppression of T(ω) at about 18000 cm^{-1} is due to the HOMO-LUMO (lowest unoccupied molecular orbital) gap. The gap probed by IR, the phonon frequencies and the overall transmission level are all anisotropic within the ab-plane. We investigated changes of the IR transmission through the entire OFET structure (Fig. 1a), consisting of a rubrene crystal, thin parylene dielectric and a thin-film ITO gate, as a function of the voltage applied between the source and gate electrodes (V_{GS}): $T(\omega, V_{GS})/T(\omega, V_{GS}=0V)$. Under an applied gate voltage, a pronounced suppression of the transmission of the transistor is observed. The effect is stronger for the polarization of the E vector along the b-axis of the rubrene single crystal. The voltage-induced changes of the transmission are most prominent at far-IR frequencies and are peaked near 400 cm^{-1}. The form of $T(V_{GS})/T(0V)$ traces does not appreciably change with the applied voltage, whereas the magnitude varies nearly linearly with V_{GS}. These observations suggest that the changes of IR properties of our devices are intimately related to the formation of accumulation layers both in the channel of the OFET and in the ITO gate electrode. Using IR microscopy[10] we have verified that the density of induced carriers is uniform along the channel of the OFETs studied here (see the Supplementary Information). Therefore, the two dimensional (2D) carrier density n_{2D} in our OFETs can be estimated as follows:

$$en_{2D} = C_t V_{GS} \qquad (1)$$

where C_t is the gate-channel capacitance per unit area (~2.1 nF/cm^2)[7], and e is the elementary charge.

In order to characterize the dynamical properties of charges in the electric-field-induced accumulation layer at the rubrene-parylene interface, it is imperative to extract the 2D optical conductivity $D\sigma_{rubrene}(\omega)$ of this layer. Spectra of $D\sigma_{rubrene}(\omega)$ extracted from an appropriate multilayer analysis (see the Supplementary Information) are presented in Fig. 2, whereas the $T(V_{GS}=-280V)/T(0V)$ spectra of the device generated from this model are plotted in Fig. 1a with thick gray lines. Note that the contribution of the conducting ITO gate electrode to the raw transmission data, $T(V_{GS})/T(0V)$, has a monotonic frequency dependence (Fig. 1a) in contrast to the non-monotonic form of the overall transmission change of the device.

Fig. 2 displays the optical conductivity spectra of the 2D system of field-induced quasiparticles at the rubrene-parylene interface $D\sigma_{rubrene}(\omega)$ for the polarization of the E vector along the a and b axes at several gate voltages. Similar to the raw $T(V_{GS})/T(0V)$ data, the conductivity spectra are characterized by a finite energy peak centered at around 400 cm^{-1}. At frequencies below this peak, $D\sigma_{rubrene}(\omega)$ decreases toward the DC value which has been obtained independently in DC transport measurements. In the near-IR range, $D\sigma_{rubrene}(\omega)$ is negligibly small as shown in Fig. 1a. In particular, no noticeable features

were observed in $\Delta\sigma_{rub}(\omega)$ at frequencies close to the band gap of rubrene. The anisotropy of the conductivity spectra is found throughout the IR range and extends to the DC limit. Importantly, $\Delta\sigma_{rub}(\omega)$ remains finite with the temperature decreasing down to 30 K (not shown) throughout the entire IR range down to at least 80-90 cm^{-1}. We therefore conclude that no sizable energy gap opens up in the IR response of the accumulation layer formed by voltage-induced holes in rubrene.

The non-monotonic form of the conductivity spectra in Fig. 2 can be qualitatively described by the localization-modified Drude model that is commonly used to account for the IR properties of organic systems and other disordered conductors in the vicinity of the metal-insulator transition[11-14]. This description is not unique. We therefore will focus on the overall strength of the absorption associated with charge injection in the accumulation layer. This analysis will allow us to evaluate the optical effective masses m* of the field-induced quasiparticles using the model-independent oscillator strength sum rule[15],

$$\frac{n_{2D}}{m^*} = \frac{2}{\pi e^2}\int_0^{\omega_c} \Delta\sigma_{rub}(\omega)d\omega \,. \qquad (2)$$

The cutoff frequency ω_c is chosen to be 5000 cm^{-1} to accommodate the entire energy region where voltage-induced changes are prominent. Exploring the results inferred through Eq. (2) we first point out that n_{2D}/m^* linearly increases with V_{GS} for both E ∥ a and E || b data (insets in Fig. 2). This is in accord with Eq. (1) provided that the effective mass does not change within the range of applied biases. This agreement of the n_{2D}/m^* data with the capacitive model justifies the use of Eq. (1) for extracting the charge density in the accumulation layer, which approaches $3.7\cdot10^{12}$ cm^{-2} at -280 V. The slopes of $n_{2D}/m^*(V_{GS})$ for the E || a and E ∥ b measurements are different as shown in Fig. 2. The latter effect in conjunction with Eqs. (1), (2) yields the anisotropy of the effective mass: $m_a^* = 1.85m_e$ and $m_b^* = 0.80m_e$. The direct spectroscopic observation of the mass anisotropy elucidates the origin of the direction dependence of the electronic mobility $\mu = e\tau/m^*$ discovered through transport measurements[6-9]. Indeed the magnitude of the anisotropy of m* is in good agreement with that of the mobility; this suggests that the effective mass of mobile quasiparticles, and not the relaxation time τ, is ultimately responsible for directional dependence of transport properties.

To understand the experimental data, we have carried out first-principles density functional theory (DFT) calculations (see the Supplementary Information) of the band structure of rubrene within the generalized gradient approximation (GGA)[16, 17], as displayed in Fig. 3. The HOMO band curvatures along the Γ-X direction and the Γ-Y direction give rise to effective masses of $1.90m_e$ and $1.29m_e$ for the hole carriers along the a and b direction, respectively, which are comparable to effective masses of the field-induced quasiparticles inferred from the above IR measurements. Therefore, our IR study along with band structure calculations reveal no significant enhancement of the effective mass of the quasiparticles in rubrene OFETs compared to the band values.

Experimental studies of charge dynamics in rubrene OFETs augmented with the analysis of the electronic structure unveil several unexpected aspects of the quasiparticles in these systems. First, no low-energy gap in the optical conductivity $D s_{rub}(w)$ is observed over the whole IR range suggesting that the field-induced quasiparticles reside in a continuum of electronic states extending both above and below the Fermi energy. The states involved in quasiparticle dynamics reflect the intrinsic electronic structure of rubrene with rather distinct values of overlap integrals in the a- and b-directions. This conclusion is attested by the anisotropy of transport properties, IR conductivity and most importantly by the effective masses directly determined from the spectroscopic data. Rather small values of effective masses of mobile quasiparticles once again point to the involvement of band states (within the HOMO band) in the electronic response in accord with the band structure analysis. These findings suggest that the periodic potential of the molecular crystal lattice and the electronic band structure play a dominant role in charge dynamics even at room temperature. Because organic molecular crystals are periodic systems, the concept of energy bands in these systems at sufficiently low temperatures is not in dispute. However, in view of weak van-der-Waals forces bonding together molecules in these crystals, the long-range order may be disrupted by the thermally-induced dynamic disorder[18]. Nevertheless, our results show that the band dispersion evaluated in the limit of $T \rightarrow 0$ provides an accurate account of transport and IR properties at room temperature. The notion of light quasiparticles in the HOMO band established through these findings is furthermore supported by recent observations of non-activated, diffusive charge transport on the surface of high-quality molecular crystals[6-9], also suggesting the existence of extended electronic states.

Light effective masses comparable to band values reported here have not been foreseen by theoretical models commonly postulating very strong coupling between electronic and lattice degrees of freedom in molecular solids leading to the formation of small polarons even at room temperature. Small polarons are characterized by large masses of at least several times the band mass due to the coupling with lattice[4,5] in stark contrast with our observations. Therefore, our work indicates that polaronic effects in rubrene OFETs are weaker at room temperature than previously thought, and the charge transport can be adequately described by quasiparticles in the HOMO band. This assertion is furthermore supported by the frequency dependence of the optical conductivity. Polarons in organic systems (including OFETs) typically give rise to broad resonances in the absorption spectra in mid-IR frequencies[10] that are not detected in our data for rubrene-based transistors. We conclude that the polaron binding energies in rubrene must be below 26 meV, the energy that corresponds to room temperature. Future work will be aimed at establishing if polaronic effects in general, and enhancement of the effective mass in particular, may be responsible for a rapid suppression of the conductivity below 140 K[8].

Methods

FET fabrication and infrared measurements

In the OFET devices investigated in this work, source and drain graphite or silver paint contacts were prepared on the surface of a rubrene single crystal followed by the deposition of approximately 1 μm of parylene which serves as the gate insulator[7]. The gate-channel capacitance per unit area C_t in this type of devices is ~2.1 nF/cm^2. As a gate electrode, we used a 24-nm-thick layer of $InSnO_x$ (ITO) with the electron density $5 10^{20}$ cm^{-3} and the sheet resistance 300 Ω/square, deposited by a dc-magnetron sputtering in pure argon. The gate electrode covers the entire device area (up to 3x3 mm^2). We investigated the IR response of numerous transistors with typical DC transport mobility $\mu \cong 5$ cm^{2}V^{-1}s^{-1} at room temperature. The absorption of the nanometer-thick accumulation channel in organic transistors is expected to be very small. In order to accurately resolve the parameters of the accumulation layer, it is crucial to minimize the contribution of the gate electrode to the overall transmission through the device. The use of ITO, much more transparent in the IR spectral range than most of the common metals, assured high transparency of our OFETs and therefore enabled spectroscopic studies of the electric-field-induced accumulation layer in rubrene from far-IR up to 2.2 eV, the HOMO-LUMO gap of rubrene.

In our IR measurements, free-standing rubrene OFETs were illuminated through the gate electrode with linearly polarized light over the frequency range 30 - 18000 cm^{-1} (4 meV-2.2 eV) with a spectral resolution of 4 cm^{-1} using a home-built set-up for broad band micro-spectroscopy. We investigated the IR transmission of the OFETs, $T(\omega, V_{GS})$, as a function of the frequency ω and the voltage applied between the source and gate electrodes, V_{GS}. The source and drain electrodes were held at the same potential in most measurements. The IR spectra depicted in Fig. 1 were obtained with the **E** vector along the a axis and b axis of rubrene at 300K. Similar spectral characteristics were found in all devices we investigated.

After this study has been completed, we became aware of the publication by M. Fischer *et al.*[19] reporting on IR properties of rubrene based OFETs. While one can recognize evident similarities in the raw data reported here and by Fisher et al, there are substantial differences in the analysis. Among them is the assessment of the role of the accumulation layer in the gate electrode in the raw data. We find that at least in the case of ITO, the voltage-induced changes of the charge density in the gate electrode dominate the response of the entire structure and have to be properly taken into account before the optical constants can be quantitatively analyzed (see the Supplementary Information).

References:

1. Malliaras, G. & Friend, R.H. An Organic Electronics Primer. *Phys. Today* 58, 53-58 (2005).

2. Forrest, S.R. The path to ubiquitous and low-cost organic electronic appliances on plastic. *Nature* 428, 911-918 (2004).

3. Dimitrakopoulos, C.D. & Malenfant, P.R.L. Organic Thin Film Transistors for Large Area Electronics. *Adv. Mater.* 14, 99-117 (2002).

4. Silinsh, E. A. & Capek, V. *Organic Molecular Crystals: Interaction, Localization, and Transport Phenomena* (AIP Press, New York, 1994).

5. Pope, M. & Swenberg, C. E. *Electronic Processes in Organic Crystals and Polymers* 2nd ed., (Oxford University Press, New York, London, 1999).

6. Gershenson, M.E., Podzorov, V., & Morpurgo, A. F. Colloquium: Electronic transport in single-crystal organic transistors. *Rev. Mod. Phys.* 78, 973-989 (2006).

7. de Boer, R.W.I.. Gershenson, M.E., Morpurgo, A.F., & Podzorov, V. Organic single-crystal field-effect transistors. *Phys. Status Solidi A* 201, 1302-1331 (2004).

8. Podzorov, V. *et al*. Intrinsic Charge Transport on the Surface of Organic Semiconductors. *Phys. Rev. Lett.* 93, 086602 (2004).

9. Podzorov, V., Menard, E., Rogers, J. A., & Gershenson, M.E. Hall Effect in the Accumulation Layers on the Surface of Organic Semiconductors. *Phys. Rev. Lett.* 95, 226601 (2005).

10. Li, Z. Q. *et al*. Infrared Imaging of the Nanometer-Thick Accumulation Layer in Organic Field-Effect Transistors. *Nano Lett.* 6, 224-228 (2006).

11. Lee, K., Heeger, A. J., & Cao, Y. Reflectance of polyaniline protonated with camphor sulfonic acid: Disordered metal on the metal-insulator boundary. *Phys. Rev. B* 48, 14884-14891 (1993).

12. Tzamalis, G., Zaidi, N. A., Homes, C. C., & Monkman, A. P. Doping-dependent studies of the Anderson-Mott localization in polyaniline at the metal-insulator boundary. *Phys. Rev. B* 66, 085202 (2002).

13. Mott, N. F. & Kaveh, M. Metal-insulator transitions in non-crystalline systems. *Adv. Phys.* 34, 329-401 (1985).

14. Mott, N. F. *Metal-Insulator Transitions* (Taylor & Francis, New York, 1990).

15. Wooten, F. *Optical Properties of Solids* (Academic, New York/London, 1972).

16. Becke, A.D. Density-functional exchange-energy approximation with correct asymptotic behavior. *Phys. Rev. A* 38, 3098-3100 (1988).

17. Lee, C., Yang, W., & Parr, R.G. Development of the Colle-Salvetti correlation-energy formula into a functional of the electron density. *Phys. Rev. B* 37, 785-789 (1988).

18. Troisi, A. & Orlandi, G. Charge-Transport Regime of Crystalline Organic Semiconductors: Diffusion Limited by Thermal Off-Diagonal Electronic Disorder. *Phys. Rev. Lett.* 96, 086601 (2006).

19. Fischer, M., Dressel, M., Gompf, B., Tripathi, A.K., & Pflaum, J. Infrared spectroscopy on the charge accumulation layer in rubrene single crystals. *Appl. Phys. Lett.* 89, 182103 (2006).

This work is supported by the NSF and DOE. Research at Rutgers University has been supported by the NSF grants DMR-0405208 and ECS-0437932. The Advanced Light Source is supported by the Director, Office of Science, Office of Basic Energy Sciences, of the U.S. Department of Energy under Contract No. DE-AC02-05CH11231.

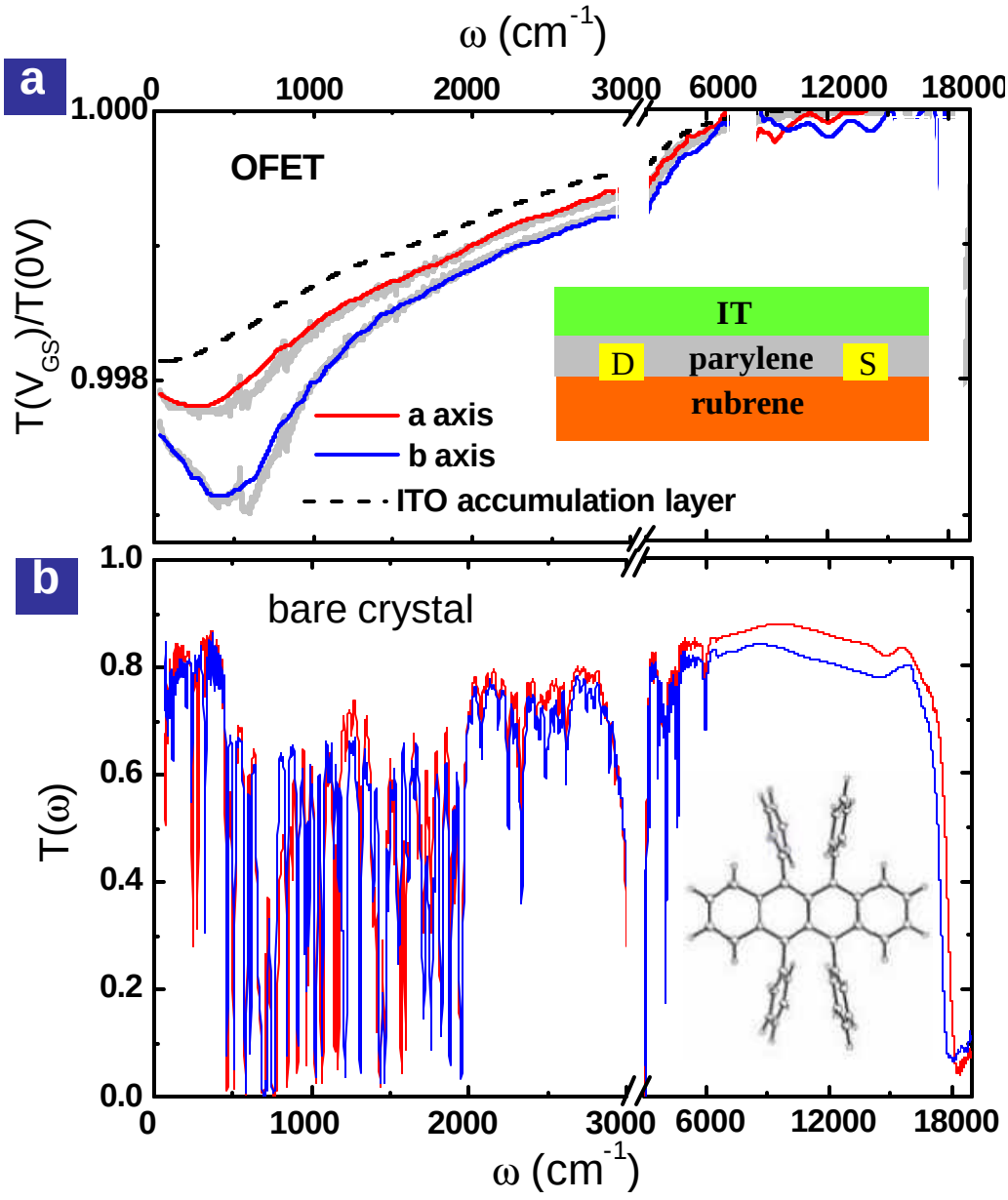

Fig 1: **The voltage-induced changes of the transmission of a rubrene OFET and transmission spectra of bare rubrene crystal. a**: voltage-induced changes of the

transmission spectra $T(\omega, V_{GS})/T(\omega, V_{GS}=0V)$ for a representative rubrene OFET device at V_{GS}=-280V. Thick gray lines: model spectra at -280V obtained from a multilayer analysis as described in the Supplementary Information. Dash line: the contribution of the accumulation layer at the ITO-parylene interface to the raw $T(\omega, V_{GS})/T(\omega, V_{GS}=0V)$ spectra obtained by omitting the rubrene accumulation layer from the multilayer model. This result shows that 0.3% increase of electron density in ITO at the largest absolute value of V_{GS} (-280 V) results in a measurable change in the transmission. **Inset of a**: a schematic of the cross-section of the OFET devices. **b**, the transmission spectra $T(\omega)$ of a bare rubrene crystal. **Inset of b**: the molecular structure of rubrene.

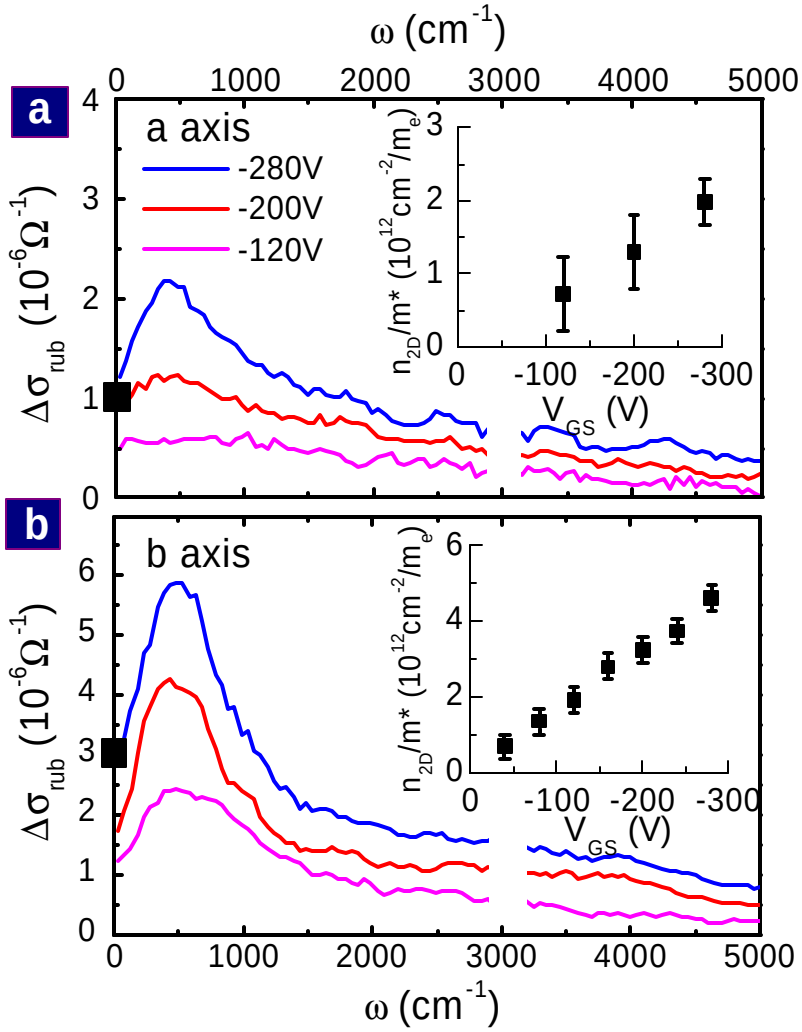

Fig 2: **The optical conductivity of the two-dimensional system of field-induced charges on the rubrene-parylene interface** $D s_{rub}(w)$ **for different values of gate voltage** V_{GS} **at room temperature. a**: E || a-axis data. **b**: E || b-axis data. Black squares on the left axes are

DC conductivity at -280V. **Insets**: the evolution of the spectral weight n_{2D}/m^* with gate voltage V_{GS}.

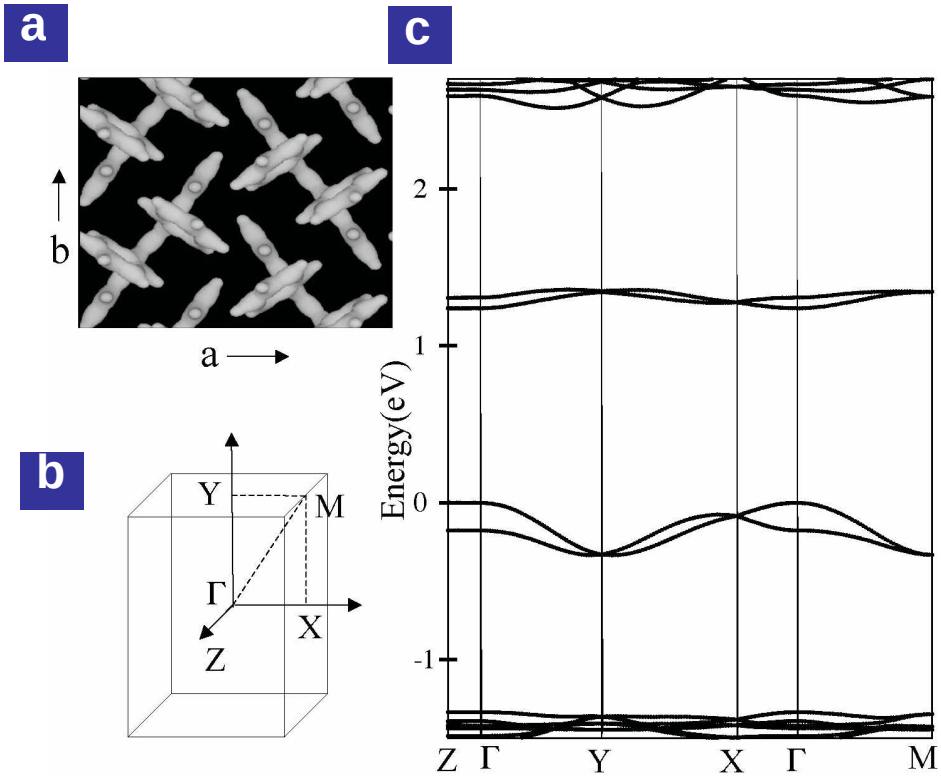

Fig 3. **The crystal structure and band structure of rubrene**. **a**: The charge density isosurface enclosing 40% of the total charges obtained from DFT calculations, which illustrates the crystal structure in the ab plane with two inequivalent rubrene molecules arranged in a herringbone structure. **b**: The corresponding reciprocal lattice; Γ-X, Γ-Y and Γ-Z correspond to the a, b and c crystalline direction. **c,** The band structure of rubrene calculated using DFT.

Supplementary Information

1: IR microscopy study of rubrene-based OFETs

In order to explore the uniformity of the charge density in our OFET devices with long channels, we carried out IR spectro-microscopy studies. Using the IR beamline 1.4.3 at the Advanced Light Source (ALS) facility, Lawrence Berkeley National Laboratory, we

were able to acquire $T(V_{GS})/T(0V)$ spectra in the range of 700-5000 cm^{-1} from individual spots at a moderate spatial resolution of 50-100 microns in diameter[1]. Since the changes of the transmission are directly related to the density of the injected charges, by scanning a focused IR beam along the conducting channel and simultaneous monitoring of $T(V_{GS})/T(0V)$, the uniformity of the accumulation layer can be studied. We observed no measurable variation in $T(V_{GS})/T(0V)$ spectra within the entire conducting channel of our devices on length scales exceeding several millimeters. This result indicates a homogeneous charge layer in rubrene-based devices without appreciable changes of the density away from the injection source/drain contacts. Previous studies of thin film OFETs have shown that the restrictions on the latter length scale only occur as the result of charge leakage through the gate insulator[1]. All rubrene-based OFETs that we have investigated so far reveal small leakage currents through the parylene dielectric consistent with the notion of macroscopically uniform accumulation layer. The macroscopic length scale of charge injection indicates that rubrene-based transistors operate similar to "ideal" FETs[1], which is further supported by the linear dependence of carrier density on gate voltage shown in the main text. Therefore, the two dimensional (2D) carrier density n_{2D} can be obtained from the capacitive model: $en_{2D} = C_i V_{GS}$, as discussed in the main text.

2: The protocol for extracting the optical constants of the accumulation layer at the rubrene-parylene interface

In order to extract the *optical constants* of the electric-field-induced accumulation layer at the rubrene-parylene interface, we employ an analysis protocol that takes into account properties of 5 layers in our devices: 1) ITO, 2) accumulation layer at the ITO-parylene interface characterized with the 2D conductivity $Ds_{ITO}(w)$, 3) parylene, 4) accumulation layer at the rubrene-parylene interface with the 2D conductivity $Ds_{rub}(w)$ and 5) the bulk of rubrene crystal. The response of layers 1, 3 and 5 was assumed to be voltage independent whereas layers 2 and 4 reveal voltage-dependent properties as indicated by the raw data in Fig. 1 of the main text. We first evaluated the complex dielectric function $e(\omega)=e_1(\omega)+ie_2(\omega)$ (related to conductivity as $e(w) = 1 + 4pis(w)/w$) for layers 1,3, and 5 from a combination of reflection, transmission and ellipsometric measurements, as depicted in Fig. S1. We then extracted $Ds_{ITO}(w)$ from the Drude model: $Ds_{ITO}(w) = \frac{n_{2D}e^2}{m^*}\frac{g_D}{g_D^2 + w^2}$, where the relaxation rate $?_D$ =1300 cm^{-1} and effective mass $m^*=0.5\ m_e$ was determined from the measurements of ITO films, and carrier density n_{2D} of ITO accumulation layer was obtained from Eq. (1) of the main text. Finally, we utilized a multi-oscillator fitting procedure[2] to account for $Ds_{rub}(w)$. In this final step the transmission of the device is calculated using standard methods for multi-layered structures taking proper account for the phase coherence of all the layers[3]. Spectra of $Ds_{rub}(w)$ extracted using this routine are presented in Fig. 2 of the main text. We conclude the description of the analysis protocol by pointing out that the response of our devices is well described by an equation written in the

spirit of Eq. (3) in Ref. 4. This equation directly relates the raw $T(V_{GS})/T(0V)$ data to 2D conductivity of the accumulation layers as:

$$1 - \frac{T(V_{GS})}{T(0V)} = \frac{2(Ds_{rub}(w) + Ds_{ITO}(w))}{Y_0 + Y_1 + Y_2 + Y_3}$$

Here Y_0 is the admittance of vacuum $1/377\Omega^{-1}$, Y_1, Y_2 and Y_3 are real parts of the admittances $[\varepsilon(\omega)]^{1/2}/377$ of each of the elements of a FET device. The spectrum of $Ds_{rub}(w)$ inferred from the above equation agrees with the modeled data with an accuracy better than 10 %, which is comparable to the error in the raw data.

3: Density functional theory calculations of the band structure of rubrene

First-principles density functional theory (DFT) calculations of the band structure of rubrene were carried out within the generalized gradient approximation (GGA). Common density functionals such as the GGA that is used in this work do not account for van der Waals forces which determine the correct distance between molecules. However, this deficiency has negligible effect on the electronic dispersion which is mainly determined by the electronic properties. We have adopted the experimental lattice parameters[5,6] (i.e., a = 14.44 Å, b = 7.18 Å, and c=26.96 Å) in our calculations. The orthorhombic unit cell contains two inequivalent rubrene molecules arranged in a herringbone structure along the basal a-b plane. There are two a-b planes in the unit cell separated by half-unit cell in the c direction which is perpendicular to the a-b plane[5,6], each contains two rubrene molecules. We find however that the interactions between the ab planes in the unit cell are negligible. The calculated electronic band dispersion is displayed in Fig. 3. The calculated band gap is about 1.24 eV, approximately half of the value determined from the absorption spectrum, as expected in the GGA to DFT calculations. The LUMO and HOMO bands near the band gap split into pairs due to the interaction of the two rubrene molecules in the ab plane. The width of the HOMO band is about 0.33eV. These results are in agreement with those previously calculated for rubrene[7] as well as for the structurally related pentacene[8,9].

References

1. Li, Z. Q. *et al.* Infrared Imaging of the Nanometer-Thick Accumulation Layer in Organic Field-Effect Transistors. *Nano Lett.* 6, 224-228 (2006).

2. Kuzmenko, A. B. Kramers–Kronig constrained variational analysis of optical spectra. *Rev. Sci. Instrum.* 76, 083108 (2005).

3. Azzam R.M. A., & Bashara, N.M. *Ellipsometry and Polarized Light* (North-Holland, Amsterdam, 1977).

4. Tsui, D.C. *et al.* High frequency conductivity in silicon inversion layers: Drude relaxation, 2D plasmons and minigaps in a surface superlattice. *Surface Sci.* 73, 419-433 (1978).

5. Kafer, D., & Witte, G. Growth of crystalline rubrene films with enhanced stability. *Phys. Chem. Chem. Phys.,* 7, 2850-2853 (2005).

6. Menard, E. *et al*. Nanoscale Surface Morphology and Rectifying Behavior of a Bulk Single-Crystal Organic Semiconductor. *Adv. Mater.* 18, 1552-1556 (2006).

7. da Silva Filho, D.A., Kim, E.-G. & Brédas, J.-L. Transport Properties in the Rubrene Crystal: Electronic Coupling and Vibrational Reorganization Energy. *Adv. Mater.* 17, 1072-1076 (2005).

8. Brocks, G., van den Brink, J. & Morpurgo, A. F. Electronic Correlations in Oligo-acene and -Thiopene Organic Molecular Crystals. *Phys. Rev. Lett.* 93, 146405 (2004),

9. Tiago, M.L., Northrup, J.E. & Louie, S. G. *Ab initio* calculation of the electronic and optical properties of solid pentacene. *Phys. Rev. B* 67, 115212 (2003).

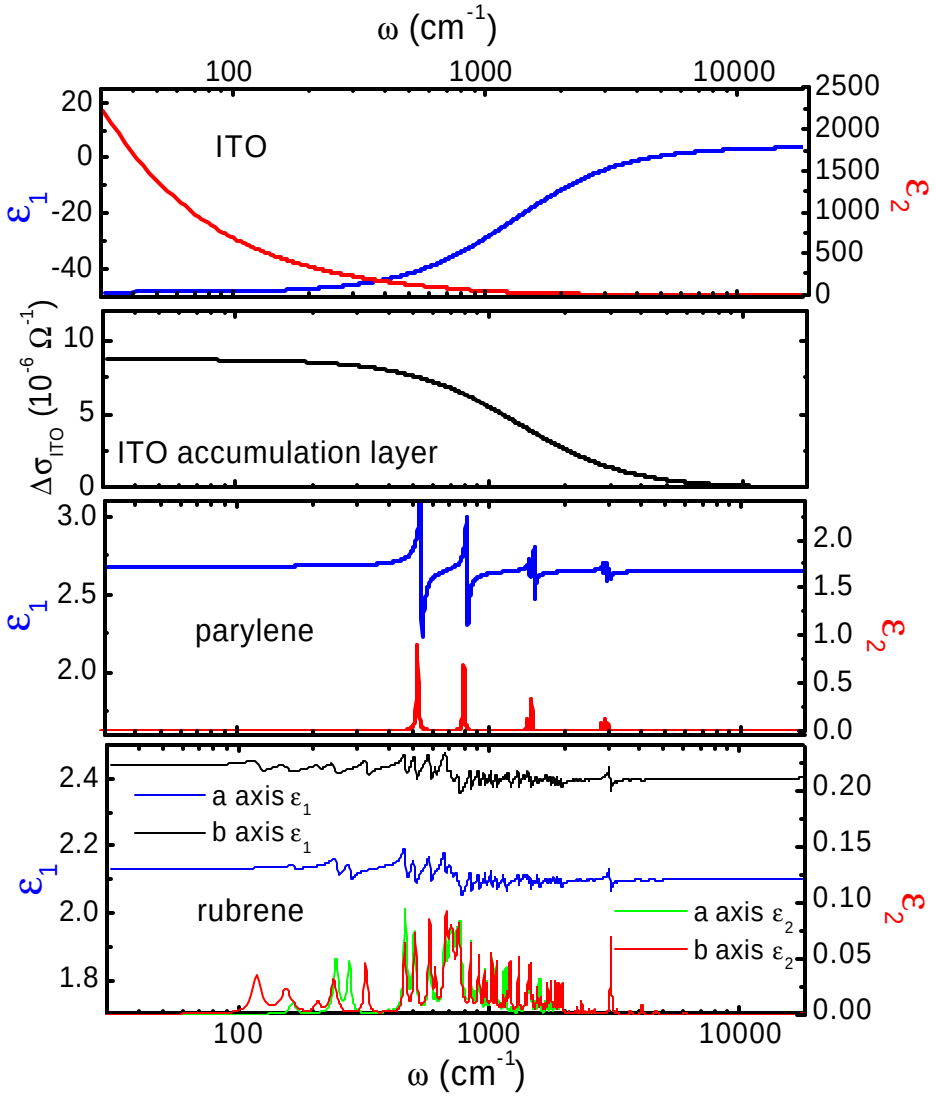

Fig. S1: Optical constants of all constituent layers in rubrene OFETs including the conductivity of the ITO accumulation layer $\Delta s_{ITO}(w)$ at V_{GS}=-280V.